RESEARCH ARTICLE
Editor's Choice
Macromolecular Chemistry and Physics
www.mcp-journal.de

Impact of Swelling on Macroscopic and Nanoscopic Mechanical Properties of Amphiphilic Polymer Co-Networks in Non-Selective and Selective Solvents

*Nora Fribiczer, Kevin Hagmann, Carolin Bunk, Frank Böhme, Regine von Klitzing, and Sebastian Seiffert**

Amphiphilic polymer gels show environmentally sensitive mechanical properties depending on the solvent polarity, which makes them useful for applications in soft contact lenses, membranes, drug delivery systems, and tissue engineering. To rationally design the material properties for such applications, a sound knowledge about the mechanical properties at different solvency states is necessary. To acquire such knowledge, amphiphilic networks are prepared by hetero-complementary coupling of amine-terminated tetra-poly(ethylene glycol) (t-PEG-NH_2) with 2-(4-nitrophenyl)-benzoxazinone terminated tetra-poly(ϵ-caprolactone) (t-PCL-Ox). The mechanical properties are investigated on different length-scales and under non-selective and selective solvent conditions using shear rheometry and atomic force microscopy (AFM). The swelling as well as the modulus in good solvent are in accord with scaling laws found for other four-arm star-shaped polymer networks and theoretical predictions. The swelling in selective solvent reveals a concentration-independent volume swelling degree and a nearly linear scaling of the modulus with concentration. The surface topography probed by AFM reveals microphase-separated structures in the range of 20 nm. Similar modulus values are obtained for bulk films in water using the complementary methods of atomic force microscopy and rheometry. The data are compared with pure hydrophilic networks to identify the effect of amphiphilicity on the material properties.

1. Introduction

Amphiphilic polymer co-networks (APCNs) are composed of both hydrophilic and hydrophobic parts that independently swell in water and organic solvents.[1] The swollen networks show environmentally sensitive viscoelasticity and selective permeability, allowing the transport of hydrophilic and hydrophobic substances to be controlled. For this reason, APCNs are most commonly used in soft contact lenses[2,3] and are excellent candidates for use as membranes,[4] drug delivery systems,[5–7] and in tissue engineering.[7,8] Among others, amphiphilic networks consisting in part of poly(ethylene glycol) (PEG) or poly(ϵ-caprolactone) (PCL), have been described in many research articles focusing on biomedical applications.[5,9]

To enable targeted materials design for these and other applications, a profound knowledge of the interplay between structural changes and resulting properties under different environmental and network-preparation conditions is essential. To investigate such structure-property

N. Fribiczer, S. Seiffert
Department of Chemistry
Johannes Gutenberg-University Mainz
Duesbergweg 10–14, D-55128 Mainz, Germany
E-mail: sebastian.seiffert@uni-mainz.de

K. Hagmann, R. von Klitzing
Institute for Condensed Matter Physics
Technical University Darmstadt
Hochschulstraße 8, D-64289 Darmstadt, Germany

C. Bunk, F. Böhme
Macromolecular Chemistry
Leibniz-Institute for Polymer Research Dresden e.V.
Hohe Straße 6, D-01069 Dresden, Germany

C. Bunk
Organic Chemistry of Polymers
Technical University Dresden
D-01062 Dresden, Germany

The ORCID identification number(s) for the author(s) of this article can be found under https://doi.org/10.1002/macp.202300389

DOI: 10.1002/macp.202300389

relations, model networks with a defined starting structure are advantageous. A powerful approach to obtain such model networks was popularized by Sakai et al.[10] utilizing hetero-complementary coupling of tetra-poly(ethylene glycol) (t-PEG) star polymers to obtain model networks with minimal network defects.[11,12] The hetero-complementary coupling based on click-chemistry prevents the formation of intramolecular loops and leads to a nearly homogeneous structure, as confirmed by Lange et al.[13] with NMR and Monte-Carlo simulations.[11,14] Despite the presence of pending arms and double links with adjacent star polymers, networks synthesized by this procedure show outstanding homogeneity and enhanced mechanical properties.[10,12,15]

This model-network-approach was also extended to amphiphilic networks. Hiroi et al.[16] combined t-PEG with linear poly(dimethyl siloxane) (PDMS) to form an amphiphilic network, which showed microphase-separation in water. The microphase-separated structure varied with the polymer volume fraction of PDMS from core-shell to lamellar morphologies. Nakagawa et al.[17] studied the structure of thermo-responsive networks prepared from tetra-poly(ethyl glycidyl ether-*co*-methyl glycidyl ether) (t-PEMGE) and t-PEG with neutron scattering and showed that the swelling degree of the network can be tuned by the network composition. Apostolides et al.[18] utilized hydrophilic t-PEG with hydrophobic tetra-poly(vinylidene fluoride) (t-PVDF) to form near-model amphiphilic co-networks. The swelling degree was found to be dependent on solvent quality, and characterization of the networks in the selective solvent water revealed the formation of hydrophobic clusters. Selective solvent here means that the solvent is a good one for the hydrophilic part and a bad one for the hydrophobic part of the network. An informative overview of the development in the field of amphiphilic polymer networks is given in a book by Patrickios.[2]

In 2022, Bunk et al.[19] presented the synthesis of a t-PEG and tetra-poly(ϵ-caprolactone) (t-PCL) based APCN in the non-selective solvents tetrahydrofuran, toluene, and chloroform, that is, good solvents for both star polymer types. Despite the hetero-complementary coupling reaction, a notable number of double links was found in the networks, which was attributed to possible specific interactions of the aromatic oxazinone terminal groups promoting the formation of double links. The double link fraction decreased with increasing polymer volume fraction. Nevertheless, an overall model-like network structure was stated due to the good agreement with a three-component fit of the data, which was used in previous work on t-PEG networks. First rheological investigations at preparation conditions were presented and connected to NMR-studies as well as theoretical calculations by Lang et al.[20] The overall scaling of the modulus with polymer volume fraction was found to be in accord with previous findings for t-PEG gels,[21] although the modulus was nearly a factor of 4 below the expectations from the phantom network model.[19,20] Furthermore, gel films based on the system of Bunk et al.[19] were studied by AFM.[22] The preparation method of the films was recognized to distinctly influence the elastic moduli found. Thin films prepared by spin coating showed a tenfold higher modulus in the selective solvent water and nearly a fourfold higher modulus in the non-selective solvent toluene compared to films obtained through bulk synthesis. This finding was explained by the drying process during spin coating, which induces the proceeding reaction of the network components resulting in crosslinking of different network levels. This leads to an overall tighter network that exhibits a lower degree of swelling and higher elastic moduli.

However, up to now, no systematic characterization of the mechanical properties on different length scales, that is, from macroscopic over microscopic to nanoscopic scales at the swelling equilibrium was presented, neither in a non-selective solvent nor in the selective solvent water. This is detrimental, as data in water are of particular interest for potential applications.

In this work, we aim to close this gap by investigating the impact of different synthesis and environmental conditions on the mechanical properties by shear rheometry and atomic force microscopy. These complementary methods provide a characterization on different length-scales to identify possible heterogeneities at the micro- and nanoscopic level and potential micro- and nanophase-separation effects at the surface. The PEG–PCL networks studied correspond to those described by Bunk et al.[19] and are based on star polymers with 10 kg mol^{-1} each. Our aim is to extend this previous work by investigating the swollen gel state and to gain interesting insights by comparing them with PEG–PEG networks also based on star polymers with 10 kg mol^{-1} each. The networks are synthesized in the non-selective solvent toluene at different temperatures and concentrations, subsequently swollen to equilibrium, dried, and transferred either back to toluene to identify the impact of drying or to the selective solvent water. The PEG–PEG networks are used to show the influence of the hydrophobic PCL part on the swelling capacity and the mechanical properties. Furthermore, swelling degree and mechanical properties are compared with predictions from theoretical models to demonstrate consistency with previous work on these systems and in general networks based on the t-PEG approach.

2. Results and Discussion

2.1. Network Formation

Prior to the study of swollen gels, the network formation of PEG–PCL gels is studied by shear rheometry in toluene and compared with NMR studies in d_8-THF.[19] For this purpose, stock solutions of the star polymers are prepared at the respective concentrations, mixed in stochiometric ratio and applied onto the rheometer, which is preheated to the synthesis temperature. The gelation is investigated at 25, 40, and 60 °C. The network formation takes place according to **Scheme 1** by hetero-complementary coupling of benzoxazinone functionalized t-PCL with amino functionalized t-PEG. The overlap concentration c^* of the polymers was determined in previous work[19] and a concentration of 70 g L^{-1} was chosen to ensure overlap of both type of star polymers. Since this work uses the same polymeric system, we adapt this and analyze networks synthesized in the concentration range $c = 70$; 140; 210; 280; 350 g L^{-1} corresponding to roughly 1–5c^*. The corresponding polymer volume fractions at preparation, ϕ_0, range from $\phi_0 = 0.06$–0.3. The network formation in this work is solely carried out in toluene.

The received gel points are summarized in **Figure 1**a and are estimated as the crossover of storage (G') and loss modulus (G'') during the course of gelation (see Figure 1b). Values with the suffix NMR are based on NMR spectroscopic monitoring of the

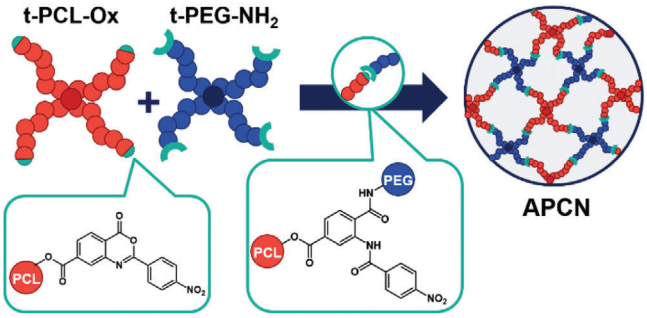

Scheme 1. Schematic reaction of t-PCL-Ox with t-PEG-NH_2 to form an APCN.

crosslinking reaction (with permission from ref. [19]).The gel point shifts to shorter timescales with increasing concentration and temperature, which is in line with expectations. Compared to the data from NMR studies in d_8-THF, the rheological gel point is shifted on the time scale by a factor of 1.1–1.5 to longer times. This discrepancy between the gel point from NMR and rheometry decreases with increasing synthesis temperature. This can be attributed to the choice of solvent: Bunk et al.[19] already stated that the kinetics are slower in toluene than in THF. Also, a different methodology is used and the intersection of storage and loss modulus represents only an upper estimate of the network formation time.[23] Nonetheless, the gel points of both methods and solvents are in semi-quantitative agreement and in the same order of magnitude.

2.2. Swelling Properties

2.2.1. Non-Selective Solvent

In the following, we consider the influence of preparation conditions on the swelling degree of PEG–PCL and PEG–PEG networks in the non-selective solvent toluene. Throughout this work, we solely consider the volume swelling degree defined as $Q = 1 + (\frac{\rho_p}{\rho_s})(\frac{w_s}{w_p})$ with the density of the polymer and the solvent (ρ_p and ρ_s), the weight of the polymer (w_p), and the weight of the solvent (w_s). Generally, the networks are prepared in toluene and

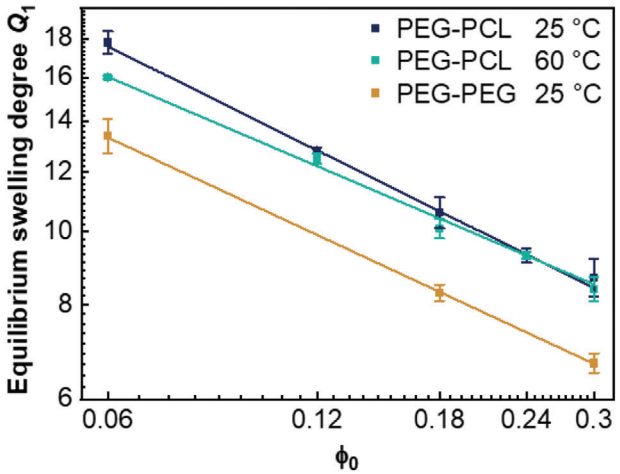

Figure 2. Average equilibrium swelling degree, Q_1, in toluene as a function of polymer volume fraction at preparation. The data follow an apparent scaling law of $Q_1 \sim \phi_0^{-\alpha}$ for all three systems, the PEG–PCL networks synthesized at 25 °C (dark blue) and 60 °C (cyan) as well as the PEG–PEG networks prepared at 25 °C (gold).

subsequently swollen to equilibrium without any drying. Afterwards, the networks are dried and reswollen in the respective solvent. For distinguishing the swelling degree before and after drying, the designations "Q_1" and "Q_2" are used accordingly. All PEG–PEG networks discussed in this publication are prepared at 25 °C.

The swelling degrees of PEG–PCL networks prepared at 25 and 60 °C range from around 8 to 18 depending on polymer volume fraction (see **Figure 2**). The networks prepared at elevated temperatures tend to have a slightly lower degree of swelling for low polymer volume fractions. However, at high polymer volume fractions, the values equalize. One possible explanation is that toluene evaporated during the network preparation, thereby increasing the polymer concentration and the concentration of reacting groups. Previously separated end groups are brought into contact, resulting in higher conversions and increased overlap between the molecules. At the same time, reactivity increases at elevated temperature. Nevertheless, the influence of the

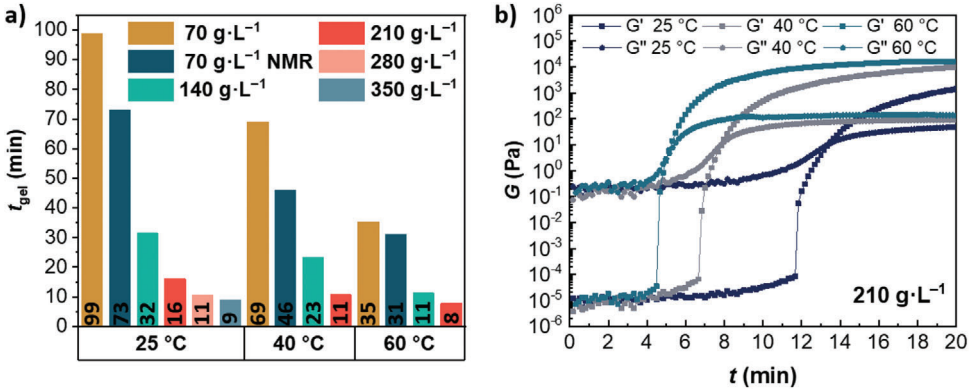

Figure 1. a) Plot of the time at the gel point against the synthesis temperature of PEG–PCL networks at different synthesis concentrations in toluene. The data marked with NMR were reproduced with permission from Bunk et al.[19] b) Exemplary plot of the recorded time sweeps for gelation at 210 g L^{-1} and 25 °C (dark blue), 40 °C (gray), and 60 °C (light blue) in toluene.

synthesis temperature on the degree of swelling is small. In accordance with our data, Bunk et al.[19] reported a degree of swelling of about 17–19 at $\phi_0 = 0.06$ and 11 at $\phi_0 = 0.18$ in toluene-d_8. This gives evidence that the used preparation and swelling procedure is consistent with the original method.

The respective degree of swelling of PEG–PEG networks in toluene prepared at 25°C range from 7 to 13 depending on the polymer volume fraction at preparation (see Figure 2). The lower degree of swelling can be attributed to the poorer solvent quality of toluene for PEG compared to PCL. This aspect was already discussed in the publication of Bunk et al.[19] based on viscosity data and the Flory-Huggins interaction parameter.

Figure 2 further shows that the plot of the average equilibrium degree of swelling, Q_1, against the polymer volume fraction at preparation, ϕ_0, follows an apparent scaling law of $Q_1 \sim \phi_0^{-\alpha}$ with $\alpha = 0.45 \pm 0.01$ for PEG–PCL prepared at 25 °C and $\alpha = 0.40 \pm 0.01$ prepared at 60 °C as well as $\alpha = 0.43 \pm 0.01$ for PEG–PEG networks. These exponents are in agreement with previous data[19] and corresponding simulations of swelling in the good-solvent regime.[20] The simulations were performed for a conversion of 95%, so the gels prepared in this experimental study must be close to this conversion. Furthermore, they follow the expectations of a scaling with $\alpha = 2/5 = 0.4$ from mean field model predictions.[24] Discrete values of the degree of swelling are noted in Table S1, Supporting Information.

2.2.2. Effect of Drying

To transfer the networks from the non-selective solvent in which they are prepared to the selective solvent, drying and reswelling is a common procedure. In this section, the influence of the drying procedure on the swelling ability of the networks is investigated as drying can increase the conversion via post-crosslinking, thus reducing the swelling capacity.

The investigated PEG–PCL gels are synthesized in toluene and dried at room temperature for five days to remove toluene. Subsequently, the networks are reswollen in toluene and the recovered swelling degree ($Q_2/Q_1 \times 100\%$) is calculated. **Figure 3** shows the recovered swelling degree for gels synthesized at 25 and 60 °C as well as for different polymer volume fractions. The results show that with the moderate way of removing the solvent, the swelling behavior of the networks hardly changes. Although the reaction conditions have an effect on the swelling behavior of the networks at low polymer volume fractions (see Figure 2), the influence on the recovery swelling degrees is only small (see Figure 3). For all networks, the second swelling in toluene almost restores the initial value, indicating that the drying procedure used does not change the network structure much. In contrast, drying at higher temperatures leads to significant changes, as evidenced by the sample synthesized at a concentration of $\phi_0 = 0.06$ and dried at 60 °C. Here, reswelling in toluene achieves only 55% of the initial swelling degree. This effect of drying at elevated temperatures (40 °C) was also shown by Bunk et al.[19] for up to three drying and reswelling cycles in tetrahydrofuran, toluene, and chloroform. The effect was particularly pronounced after the first drying and reswelling cycle and at low polymer volume fractions. Only 63–68% of the initial swelling degree was recovered in toluene at $\phi_0 = 0.06$. At higher volume fractions of $\phi_0 = 0.18$ about 90–95%

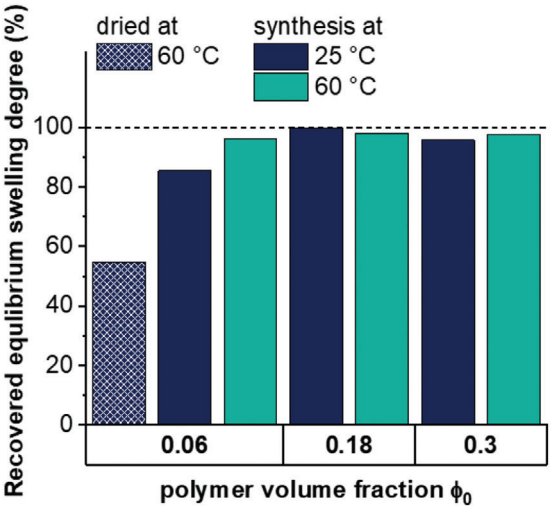

Figure 3. Recovered swelling degrees ($(Q_2/Q_1) \times 100\%$) of PEG–PCL networks synthesized at 25 °C (dark blue) and 60 °C (cyan) after respective drying procedure and reswelling in toluene. Unless stated otherwise, the gels were dried at 25 °C for five days.

recovery was observed. This shows that the relative number of free reaction groups is higher at low polymer content which leads to stronger additional cross-linking after the first drying. Apparently, post-reactions take place during drying at higher temperatures, resulting in increased network density. Nevertheless, the solvent evaporation rate has an impact on the gel structure especially during synthesis, which becomes for instance important during preparation of thin gel films (i.e., high surface/volume ratio). Hagmann et al.[22] prepared either thin films by spin coating or dried their films at 60 °C. In both cases, rapid evaporation of the solvents led to noticeable post-crosslinking, resulting in high elastic moduli. In contrast to this, we show that drying of the gels at room temperature over a longer period of time has a negligible effect on the swelling capacity especially at higher polymer volume fractions. Therefore, it is justified to compare the swelling degrees Q_1 in toluene with Q_2 in water for the PEG–PEG networks. The suitability of the presented drying procedure at room temperature is further proven by rheological measurements and comparison of the storage modulus in toluene before and after drying. The exact values of Figure 3 are included in Table S2, Supporting Information.

2.2.3. Selective Solvent

After studying the swelling of the networks in a non-selective solvent and the impact of the drying procedure, swelling in the selective solvent water is investigated, which is of particular interest due to potential applications. The networks are prepared in toluene, dried at room temperature for five days, and reswollen to equilibrium in water. The swelling degrees in water determined after drying are referred to as Q_2.

While the gels are highly swollen and transparent in toluene, they exhibit lower swelling and a cloudy appearance in water (see Figures S1 and S2, Supporting Information). This indicates clustering or colloidal behavior of the PCL star polymers due to their hydrophobicity. AFM tapping mode images of the swollen

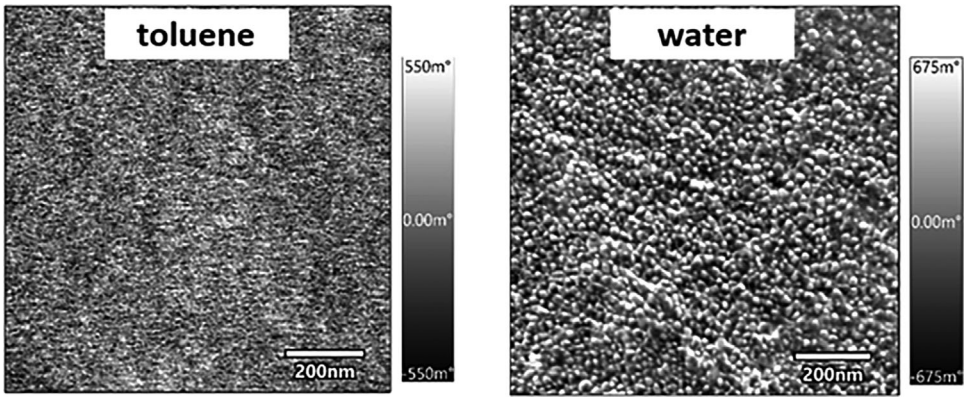

Figure 4. Surface topography of PEG–PCL gels measured with AFM in tapping mode. The phase images of the networks swollen in toluene (non-selective solvent, and non-dried) and water (selective solvent; after drying and reswelling) are displayed. In toluene, no surface structure is noticeable; in water, in turn, microphase-separation is visible in the form of nearly spherical structures covering the entire surface.

APCNs are taken to get an idea of the surface structure in toluene and the extent of microphase separation in water (see **Figure 4**). In water, the microphase-separated structure essentially resembles nearly spherical domains, which could be visualized at the surface by phase imaging in AFM (see Figure 4). The size of these domains at the surface is 20 ± 5 nm, giving evidence of the clustering of several PCL-stars. A similar average distance of roughly 19 nm between the microphase-separated domains and a radius of the domains of roughly 5–6 nm was also found in SAXS experiments on bulk gels by Löser et al., representing the aggregation of 17–25 PCL star polymers.[25] The study furthermore confirms that the PCL clusters are nearly PEG free and adapt an ellipsoidal shape. Such small length-scales are close to the resolution limit of the AFM measurements carried out in this study, since the curvature radius of the AFM tips is roughly 8 nm for imaging in tapping mode and determining mechanical properties through indentation measurements. Nevertheless, it is quite remarkable to find the same type of phase separation on the same length-scale through various methods such as SAXS and AFM. Deviations in size and shape may be attributed to differences in the analysis of bulk and surface structure.

In toluene, in contrast, no underlying structure can be detected in the AFM phase image (see Figure 4). This is consistent with the expectation, as both star-types swell in the non-selective solvent, resulting in homogeneously swollen networks on the investigated length-scale. These findings are also confirmed by height images, which show a smooth surface in toluene and a significantly rougher surface in water. The height images are provided in Figure S3, Supporting Information.

The respective swelling degrees of PEG–PCL and PEG–PEG networks in water are displayed in **Figure 5**. The PEG–PCL networks show a degree of swelling statistically scattering around 3, independent of the initial polymer volume fraction at preparation and the synthesis temperature (see Figure 5a; discrete values are included in Table S3, Supporting Information). The significantly lower values compared to swelling in toluene can be explained by the selective swelling behavior of the respective polymers PEG and PCL in water. Whereas the hydrophilic PEG tends to swell in water, the hydrophobic PCL shows the opposite tendency to contract and repel the water. Due to the 50:50 mixture in all networks investigated, these opposite tendencies of swelling and shrinking seem to balance out, resulting in a swelling degree of three. That might explain why the swelling degree of PEG–PCL gels does not depend on the polymer content.

Considering the swelling degree in water and the network composition (50:50 mixture of the star polymers), the found nearly spherical shape in Figure 4 can possibly be explained by the phase separation behavior of block copolymers, although they

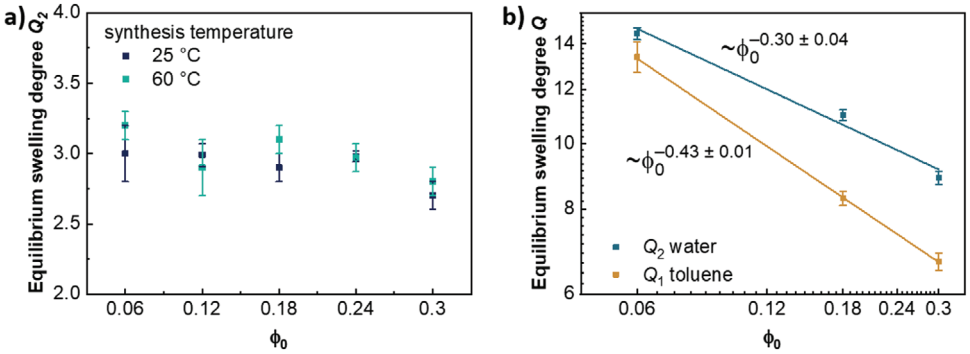

Figure 5. Equilibrium swelling degree as a function of polymer volume fraction at preparation. a) PEG–PCL gels in water synthesized at 25 °C (dark blue) and 60 °C (cyan). b) PEG–PEG networks in water (blue) and toluene (gold) synthesized at 25 °C. Since the gels were synthesized in toluene they were dried before studying them in water.

have a higher degree of freedom compared to the network. It is known from block copolymers in bulk that spherical structures are obtained at low volume fractions of one of the blocks.[26] In our case, a degree of swelling of 3 roughly translates to a total polymer volume fraction of 0.3.[27] As only half of the polymer fraction consists of PCL stars, the polymer volume fraction of PCL is about 0.15. Such small fractions of one species are assigned to the aforementioned spherical structures.[26,28]

In contrast to the PEG–PCL networks, which have a cloudy appearance in water, the PEG–PEG gels remain transparent (see Figure S1, Supporting Information). They exhibit a higher swelling degree ranging from 9 to 14.5 depending on the initial polymer volume fraction (see Figure 5b). Hence, the swelling ratio of PEG–PEG gels is much higher than that of PEG–PCL gels. This is plausible because water is a better solvent for PEG than for PCL. The PEG–PEG networks also show a degree of swelling that is 1.1–1.3 times higher in water than in toluene. Both water and toluene are in general good solvents for PEG, but the higher swelling degree in water indicates a slightly better solvent quality.

The solvent quality is often discussed in terms of the Flory–Huggins interaction parameter χ, which quantifies the interaction energies between the polymer and the solvent. Another important parameter in this context is the overlap concentration c^*, which is inversely proportional to the intrinsic viscosity $[\eta]$.[29] In turn, the intrinsic viscosity is a measure of the increase in viscosity caused by the polymer and gives an indication on the expansion of the polymer in solution. The Flory–Huggins parameter of linear PEG in water is about 0.43[30] and that of t-PEG-NH_2 was determined to be 0.465–0.495[31] depending on the molar mass. In toluene, a value of $\chi = 0.38$ was computed for t-PEG-NH_2 with 10 kg mol^{-1} from experimental viscosity data at 25 °C using the Tian–Munk model.[19,32] Based on this estimate, toluene would be the better solvent for PEG, but the swelling results indicate the opposite trend. Therefore, the overlap concentration or its reciprocal, the intrinsic viscosity, is used as a further measure of solvent quality. The overlap concentration in toluene of amine terminated t-PEG at 25 °C is $c^* = 76.2 \pm 0.5$ g L^{-1} [19] corresponding to an intrinsic viscosity of $[\eta] = 0.01312$ L g^{-1}. The value in water was determined in this work to be $c^* = 60 \pm 2$ g L^{-1} corresponding to $[\eta] = 0.01680$ L g^{-1} and agrees very well with the overlap concentration of 60 g L^{-1} determined by Sakai et al.[10] for the formation of t-PEG networks in aqueous buffer solution. According to these data, PEG is more expanded, that is, swollen, in water than in toluene. Therefore, a lower polymer concentration is required to achieve space filling.

To validate the viscosity results, they are related to the value for linear PEG chains of the same molar mass. The ratio of the intrinsic viscosity of the star polymers to that of corresponding linear polymers is called the contraction factor, which indicates that star polymers are more compact and have a lower radius of gyration than their linear analogues at the same molar mass.[33] The contraction factor describes this decrease in intrinsic viscosity due to the more compact architecture and is defined as $g_\eta = [\eta]_b/[\eta]_l$ with intrinsic viscosity of the branched four-armed star polymer, $[\eta]_b$, and the intrinsic viscosity of the linear polymer $[\eta]_l$. For four-armed star polymers in a good solvent contraction factors of $g_\eta = 0.68$–0.74[33,34] are found. In this work, we calculated a ratio of $g_\eta = 0.68$ using $[\eta]_l = 0.02486$ L g^{-1} for linear PEG (10 kg mol^{-1})[35] and the experimentally found value of $[\eta]_b = 0.01680$ L g^{-1} for t-PEG-NH_2 (10.8 kg mol^{-1}). This agrees quite well with the literature data despite the difference in molar mass and the change in end-group chemistry from hydroxy to amine end groups. In conclusion, based on the experimental viscosity data, water is the better solvent for PEG at the experimental conditions used.

Just like in toluene, the swelling degree of the PEG–PEG gels in water shows a dependency on the initial polymer volume fraction according to the apparent scaling law $Q_2 \sim \phi_0^{-\alpha}$ (see Figure 5b). The exponent of the apparent scaling law $Q_2 \sim \phi_0^{-\alpha}$ is 0.30 ± 0.04 and consequently lower than in toluene. As both toluene and water are rather good solvents for PEG, we would expect a similar exponent. The swelling degree in water was determined after drying of the gels in between for the solvent exchange from toluene to water. This might have induced some post-crosslinking reaction, leading to higher conversion and thus lower achievable swelling degree. This effect is more pronounced at lower polymer volume fractions, which results in the observed lower exponent. An additional point to keep in mind is the connection of the PEG–PEG networks by an aromatic linking group, which could affect the swelling capacity of the gels in water by clustering.

The data of the PEG–PEG gels confirm the assumption made above that the low swelling degree of PEG–PCL networks in water is mainly due to the hydrophobicity of the PCL moieties. The possible additional shrinkage tendency due to the aromatic linking group should be negligible in contrast to the shrinking induced by PCL, as the PEG–PEG gels swell more in water than in the less polar solvent toluene.

2.3. Mechanical Properties

All shear rheological and AFM measurements in this chapter were performed at equilibrium swelling and at 25 °C, if not stated otherwise.

2.3.1. Effect of Drying on Mechanics

In a first step, the drying procedure is verified by comparing the storage moduli of the gels swollen in toluene before and after drying. Storage moduli of toluene-swollen gels before (G'_1) and after the drying procedure (G'_2) as determined by rheometry are summarized in **Figure 6**. The gels are again prepared in toluene, dried at room temperature for five days, and subsequently reswollen in toluene.

For both PEG–PCL and PEG–PEG networks, the storage moduli after the drying are slightly higher, but within the margin of the error. This is in accord with the previous findings for the swelling degree, which were also not significantly influenced by the chosen drying procedure. Again, the values are independent of the chosen preparation temperature. Therefore, we conclude that this moderate drying procedure does not lead to a distinct increase in conversion due to the slow drying and is suitable for the transfer from non-selective to selective solvent.

Furthermore, it is obvious from Figure 6 that the PEG–PEG gels show a higher storage modulus compared to the PEG–PCL ones prepared at the same concentration. This is reasonable, as we observed lower swelling degrees of the PEG–PEG gels in toluene (compare Figure 2).

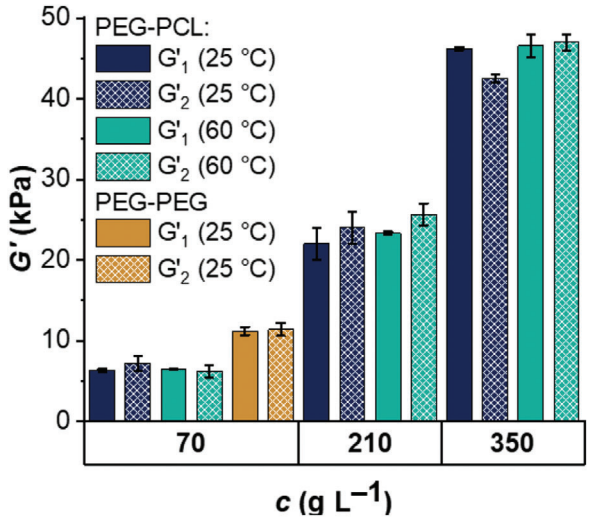

Figure 6. Rheometry measurements in toluene: Storage modulus of PEG–PCL (dark blue: synthesis at 25 °C; and cyan: synthesis at 60 °C) and PEG–PEG networks (gold: synthesis at 25 °C) at swelling equilibrium in toluene before drying, G'_1 (plane bars), and after drying for five days at room temperature, G'_2 (hatched bars).

2.3.2. Non-Selective Solvent

In a second step, the storage moduli and scaling behavior of PEG–PCL and PEG–PEG gels are discussed. The gels are prepared in toluene, subsequently swollen to equilibrium and investigated via shear rheometry and AFM.

From shear rheometry, the shear storage modulus G' as well as the shear loss modulus G'' are received directly on a macroscopic length-scale. Whereas in AFM, the elastic modulus E is obtained by static indentation measurements. As our networks are essentially elastic, we assume for the elastic storage modulus $E' \approx E$. Colloidal probes (µm-sized) are used to obtain elastic information on a larger scale, while nanoindentation with a sharp AFM-tip is performed to obtain information on very small length-scales. Respective histograms of the received elastic moduli in both types of solvent are included in Figure S4, Supporting Information.

Comparison of both methods is feasible by converting the elastic storage modulus E' to shear storage modulus G' using the relation $G' = \frac{E'}{2(1+\mu)}$ with the Poisson ratio μ.[23,27] According to literature, a Poisson ratio of $\mu = 0.5$ applies to incompressible materials, whereas Poisson ratios down to $\mu = 0.25$ are found for materials under deformation and in contact with excess solvent, which are also described in theoretical work.[36–38] In contrast, an increase in Poisson ratio was found for networks in contact with air under deformation ($\mu > 0.5$).[36] For swollen gels, values between these extremes, namely $0.25 < \mu < 0.5$, are found.[38,39] For t-PEG gels, however, it was found for biaxial deformation that the Poisson ratio is well approximated with $\mu = 0.5$,[40] which was also stated in other work comparing Young's modulus with shear modulus.[41] Furthermore, using $\mu = 0.5$ or $\mu = 0.25$ to convert the elastic modulus to shear modulus results in a factor of 1.2 lower or higher values, respectively. This factor is within the margin of error of the transformed AFM results (see Table S4, Supporting Information). Therefore, and for consistency with the AFM evaluation (see Section 4), $\mu = 0.5$ is used.

Table 1. Storage modulus of PEG–PCL networks swollen in toluene converted with a Poisson's ratio of $\mu = 0.5$ from AFM measurements with tip (radius ≈ 8 nm) and colloidal probe (CP33: radius 3.3 µm) as well as storage modulus directly from rheological measurements. The error of the converted modulus corresponds to the percentage error of the original data.

$c^{a)}$ [g L^{-1}]	G'_1 [kPa] from AFM		G'_1 [kPa] from rheometry	
	tip[b)]	CP33[b)]	25 °C[c)]	60 °C[c)]
70	9 ± 3	8 ± 1	6.3 ± 0.2	6.5 ± 0.1
140	25 ± 4	15 ± 3	13.91 ± 0.09	15.3 ± 0.2
210	31 ± 16	20 ± 6	22 ± 2	23.3 ± 0.2
280	43 ± 20	25 ± 7	34 ± 1	34.9 ± 0.3
350	79 ± 14	35 ± 7	46.2 ± 0.2	47 ± 1

[a)] Concentration at preparation; [b)] Synthesis at 60 °C; [c)] Synthesis temperature.

Table 1 summarizes the shear modulus of toluene-swollen and non-dried PEG–PCL gels received by rheometry and converted from AFM measurements with a Poisson's ratio of 0.5 for measurements with tip (tip radius ≈ 8 nm) and colloidal probes with a radius of 3.3 µm (CP33).

Both the microscopic and macroscopic derived shear moduli are approximately equal for the PEG–PCL networks swollen in toluene (see also **Figure 7**). The values obtained with the sharp tip are shifted to slightly higher values compared to the colloidal probes and the rheometry measurements, especially at high initial polymer concentration. This shift could be due to the fact that the tip geometry of the manufacturer is not exactly known and may also vary among the individual tips. To clarify this, studying the exact tip shapes via electron microscopy would be necessary. In addition, evaporation of the solvent may have occurred during the changing of the tips and sample handling, which in turn leads to harder networks. Finally, the networks are not

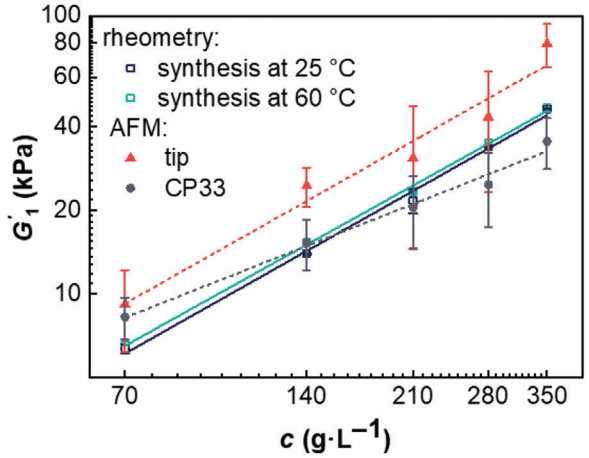

Figure 7. Storage modulus from AFM (full symbols) and rheometry (open symbols) of PEG–PCL networks swollen in toluene. Rheology measurements were conducted on gels synthesized at 25 °C (dark blue) and 60 °C (cyan). AFM measurements were performed on gels synthesized at 60 °C using a sharp tip (red triangles) or colloidal probe CP33 (grey circles).

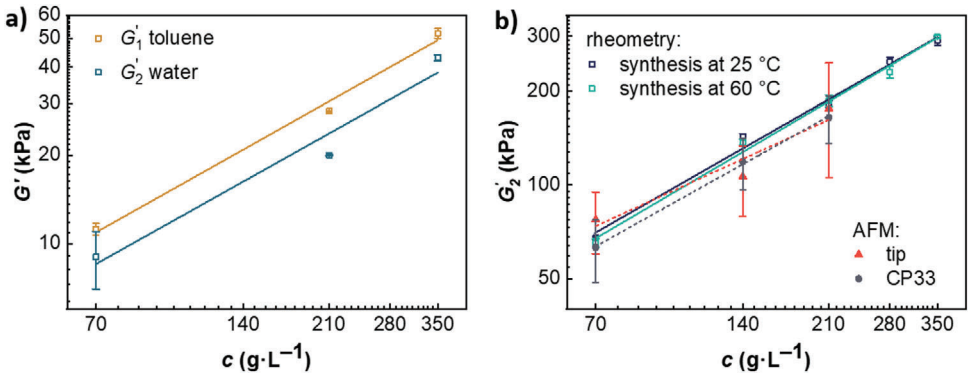

Figure 8. Storage modulus at equilibrium swelling obtained by rheometry (open symbols) and converted from AFM (full symbols) a) PEG–PEG gels in toluene (gold) and water (light blue) synthesized at 25 °C. b) PEG–PCL gels in water obtained by AFM with tip (red triangles) and colloidal probe (grey circles) for a synthesis temperature of 60 °C and by rheometry (open rectangles) for synthesis temperatures of 25 °C (dark blue) and 60 °C (cyan).

completely ideal regarding their connectivity, as shown in earlier studies by MQ-NMR[19] which may influence the modulus on these small length-scales. The overall agreement between AFM for both indenter geometries and rheology is somewhat expected since the networks are swollen in a co-solvent for both polymer types and the surface topography does not reveal any underlying structure. Consequently, the results substantiate the picture of a homogeneous swollen network.

In analogy to the swelling degree in the previous section, the storage modulus follows an apparent scaling law $G_1' \sim \phi_0^{\beta}$ as a function of initial polymer volume fraction. Figure 7 shows the storage modulus, G_1', of the PEG–PCL networks included in Table 1 in toluene as a function of concentration at network preparation.

The storage moduli obtained from rheometry show exponents of 1.23 ± 0.05 and 1.21 ± 0.03 for the networks prepared at 25 and 60 °C, respectively. The modulus converted from AFM measurements with tip follows an analogue scaling with an exponent of 1.2 ± 0.1. The results with colloidal probes scale with a nearly linear exponent of 0.86 ± 0.06. Small deviations between the methodologies are to be expected since delamination of network gel films on a macroscopic scale occurred during AFM measurements. Evaporation of solvent during sample handling contributes to sample inhomogeneities. To counteract delamination, gel films were immobilized on silicon substrates as described previously,[22] however, after some time, sample deformation still occurred and complicated the measurements independent of indenter geometry. A similar log–log slope of roughly 1.3 was found in related work on t-PEG gels in the preparation state based on precursors of 10 kg mol^{-1} [21,42] as well as in biaxial deformation of t-PEG gels based on 20 kg mol^{-1} precursors.[40] Additionally, the scaling with an exponent of 1.22 ± 0.05 was found for the PEG–PCL networks in toluene in the preparation state.[19] The exponent higher than 1 can be attributed to the following reasons: The conversion at low concentrations is somewhat lower than at high concentrations. At higher concentrations, there are fewer connectivity defects, especially double links, which reduce the modulus, and above the overlap concentration, additional effects due to entanglements may play a role.

The PEG–PEG networks, instead, show a shallower and nearly linear scaling with an exponent of 0.94 ± 0.08 (see **Figure 8**a, absolute values of modulus in Table 4). Nevertheless, the scaling with an exponent near one in case of the PEG–PEG networks is also reasonable as the modulus is proportional to the concentration of the elastically active network strands which in turn is proportional to polymer concentration. The different scaling due to the change from amphiphilic to hydrophilic networks might be attributed to a change in the factors named above. Furthermore, a higher fraction of single links was found for pure PEG–PEG networks, than for PEG–PCL networks at the overlap concentration, i.e., fewer defects result in a higher modulus.[19] Likewise, the t-PEG-Ox macromonomers show a different conformation and expansion in toluene during synthesis than their PCL analogues, which may influence the resulting gel structure. Similarly, the onset of entanglements may shift and influence the modulus. Which one of the mentioned effects is finally responsible for the shift in scaling cannot be explained yet.

In summary, it was shown that absolute numbers of modulus in toluene are comparable for rheology and AFM measurements on bulk films. The modulus in this work is three times higher compared with the modulus in the preparation state of Bunk et al., [19] despite measurement at equilibrium swelling. This is attributed to the significantly longer reaction time in this work and the resulting higher conversion, since the same scaling is seen in both cases.

To consider the efficiency of crosslinking, the number density of elastically active network strands ν is caluclated from the experimental results, ν_{exp}, and compared to the theoretical, ideally achievable value, ν_{theo}. The experimental number density of elastically active network strands can be calculated from modulus data $\nu_{exp} = \frac{G'}{0.5RT}$ and the theoretical value can be calculated from the polymer concentration at network formation under consideration of the decrease in concentration due to swelling.[18,23,43] The resulting number densities for both network types (synthesis at 25 °C) based on the rheological measurements are summarized in **Table 2**. The values received from the AFM measurements are included in Table S5, Supporting Information as they show qualitatively the same trend and are in the same order of magnitude. Furthermore, in AFM, the swelling of the gels is affected by the attachment of the networks to the silicon substrate, that is, the concentration decrease cannot be determined accurately for calculation of the theoretical expected value. Therefore, the same

Table 2. Comparison of experimentally found and theoretically calculated elastically effect chains, ν_{exp} and ν_{theo}, based on the phantom network model prediction for PEG–PCL and PEG–PEG networks in toluene at 25 °C.

c [g L^{-1}]	PEG–PCL			PEG–PEG		
	ν_{exp} [mmol L^{-1}]	ν_{theo} [mmol L^{-1}]	ν_{exp}/ν_{theo}	ν_{exp} [mmol L^{-1}]	ν_{theo} [mmol L^{-1}]	ν_{exp}/ν_{theo}
70	5.1	12.2	0.4	9.0	15.4	0.6
140	11.2	18.0	0.6			
210	17.5	22.9	0.8	22.8	27.7	0.8
280	27.4	27.4	1.0			
350	37.3	30.8	1.2	42.0	37.9	1.1

theoretical values included in Table 2 were taken as a reference for the AFM results in Table S5, Supporting Information.

Table 2 illustrates, that the crosslinking efficiency increases with concentration and reaches the maximal efficiency at four times the overlap concentration (280 g L^{-1}). This is in line with MQ-NMR studies[19] of the connectivities of such networks, revealing that the fraction of single links increases with increasing concentration, while higher order connectivities and defects decrease. The PEG–PEG networks show a slightly higher crosslinking efficiency at low concentrations compared to the PEG–PCL networks, which is also expected based on the aforementioned investigations. The ratio higher than one at 350 g L^{-1} could be the result of occurring entanglements and an accompanying increase in modulus. A further check for plausibility of the results is performed later on by comparison with the modulus from the phantom network model.

2.3.3. Selective Solvent

Investigation of the mechanical properties in the selective solvent water are of special interest, due to possible applications in this medium. All samples presented in this section are prepared in toluene, dried according to the drying procedure described above and reswollen in water to equilibrium. **Table 3** summarizes the shear moduli of PEG–PCL networks in water from rheometry and those calculated from AFM measurements with a Poisson ratio of 0.5. The total values are 7–10 times higher compared to toluene, which is a result of the lower swelling degree due to the collapse of the hydrophobic PCL parts of the network. The total values are of the same order of magnitude for both methods, AFM and rheometry, and independent of the indenter geometry used in AFM and the preparation temperatures of the networks. The error of the AFM data is significantly larger due to the rough surface and the macroscopic distortion of the sample that occurred specifically after drying and reswelling of the sample. Sample distortion is not so critical in rheometry because small discs are measured and a plate-plate geometry is used, which automatically flattened the gels to fit in the gap. In the AFM measurements, however, the distortion is on the length-scale investigated. This effect becomes more severe the higher the concentration. Therefore, measurements of 280 and 350 g L^{-1} is not possible using the AFM methodology. Additionally, the fit of the force-distance-curves is dependent on the fit-depth, indicating non-Hertzian elastic behavior of the gel film in water. All force distance curves are fitted to an indentation depth of 100 nm to obtain comparable results throughout all experiments. We attribute this non-Hertzian elastic behavior to the microphase-separated surface structure of dense PCL clusters composed of several tens of PCL star polymers surrounded by expanded PEG polymers.[25]

Table 3. Storage modulus of PEG–PCL networks swollen in water from AFM measurements with tip (radius ≈ 8 nm) and colloidal probe (CP33: 3.3 µm) converted with a Poisson's ratio of $\mu = 0.5$ as well as storage modulus directly from rheological measurements. The error of the converted modulus corresponds to the percentage error of the original data.

$c^{a)}$ [g L^{-1}]	G'_2 [kPa] from AFM		G'_2 [kPa] from rheometry	
	tip	CP33	25 °C$^{b)}$	60 °C$^{b)}$
70	77 ± 17	63 ± 14	67.5 ± 0.5	65 ± 2
140	106 ± 27	119 ± 22	143 ± 3	137 ± 3
210	176 ± 70	164 ± 28	181 ± 5	186 ± 8
280	–	–	248 ± 8	230 ± 10
350	–	–	290 ± 10	299 ± 3

[a)] Concentration at preparation; [b)] Synthesis temperature.

Due to the found microphase-separated structure in water (see Figure 3), differences in local modulus from AFM and macroscopic modulus in rheology would have been expected, as especially the AFM tip size is a similar size regime as the observed domains at the surface. These expected differences in water cannot be found in the experiment. This might be due to the circumstance that the AFM nanoindenter tip with a curvature radius of roughly 8 nm may not be sharp enough to properly observe local differences in modulus. Also, we assume that the indentation process (with an indentation depth of more than 100 nm) occurs by pushing hard PCL spheres through a soft, swollen PEG network. This process is independent of the precise starting point. In both cases, a rather averaged modulus is measured.

In analogy to the storage modulus in toluene, an apparent scaling law of modulus with polymer volume fraction $G'_2 \sim \phi_0^{\beta}$ can be observed. Figure 8 shows this dependency at swelling equilibrium in water as a function of concentration at network preparation for both PEG–PEG (a) and PEG–PCL (b) networks.

The exponent is found to be 0.90 ± 0.05 and 0.92 ± 0.04 for PEG–PCL networks prepared at 25 and 60 °C studied by rheometry. An analogue scaling with exponents of 0.7 ± 0.2 and 0.88 ± 0.03 is found for the samples studied by AFM with tip and colloidal probe. The scaling is nearly linear, which is reasonable as the modulus is proportional to the effective elastically active network strands, which are in turn proportional to the polymer concentration. Due to the concentration-independent swelling

Table 4. Calculated phantom modulus, Gph, of PEG–PCL and PEG–PEG networks as well as the experimentally received modulus, Gexp, of the PEG–PEG networks in water and toluene. The ratio of phantom modulus and experimentally obtained modulus was calculated for the networks prepared at 25 °C. The index "tol" represents toluene and the index "water" represents water.

c [g L^{-1}]	PEG–PCL		PEG–PEG				
	G_{ph} [kPa]	G_{ph}/G_{exp}^{tol}	G_{ph} [kPa]	G_{exp}^{tol} [kPa]	G_{ph}/G_{exp}^{tol}	G_{exp}^{water} [kPa]	G_{ph}/G_{exp}^{water}
70	15.2	2.4	14.4	11.2 ± 0.5	1.3	9 ± 2	1.6
140	30.4	2.2	28.9				
210	45.6	2.1	43.3	28.3 ± 0.1	1.5	20.03 ± 0.09	2.2
280	60.8	1.8	57.7				
350	76.1	1.7	72.1	52 ± 2	1.4	43 ± 1	1.7

degree of 3 in water, the polymer concentration decreases by about one third at each concentration due to swelling. However, since this is the same for all concentrations, the increase in concentration is still linear. Therefore, the concentration of the effective elastically active network strands also increases linearly and thus also the modulus.

The PEG–PEG networks also show a comparable scaling with an exponent of 0.9 ± 0.2, which is in accord with the exponent in toluene of 0.94 ± 0.08 and again nearly linear (absolute values of modulus are included in **Table 4**). This is reasonable, as both solvents are non-selective solvents for PEG and a similar scaling is to be expected.

Comparison with Phantom Model and Mesh Size Estimation: To compare our results with theory, we relate them to the expectation from the phantom network model. The phantom modulus in the investigated systems can be described as follows[19,23,27,44]

$$G_{ph} \approx \phi_0 \left(1 - \frac{2}{f}\right) \frac{\rho RT}{M_{el}} \quad (1)$$

This yields $G_{ph}/\phi_0 \approx 253.5$ kPa for PEG–PCL and $G_{ph}/\phi_0 \approx 240.4$ kPa for PEG–PEG with a functionality $f = 4$, the density of the dry network being $\rho = 1.13$ g mL^{-1} [45] on average, the universal gas constant R, the temperature $T = 298.15$ K, and the molar mass per network strand of $M_{el} \approx 5.5$ kg mol^{-1} in case of the PEG–PCL networks and $M_{el} \approx 5.8$ kg mol^{-1} in case of PEG–PEG networks, respectively. With the respective polymer volume fractions at preparation ϕ_0, the expected modulus can be estimated as $G_{ph} \approx \phi_0 \cdot 253.5$ kPa or respectively $G_{ph} \approx \phi_0 \cdot 240.4$ kPa. The resulting moduli are summarized in Table 4. We again use the rheology data for comparison as the corresponding errors are small compared to the AFM results. The comparison with the experimentally determined values in Table 1 shows that the phantom modulus is always higher than the experimental value. This can be explained by the assumptions of the model system, in which ideal crosslinking of the polymers is presupposed. However, this is not the case for the present systems due to a non-negligible amount of double links and other connectivity defects, as shown in previous work.[19] The discrepancy between phantom modulus and experimental modulus decreases for the PEG–PCL systems with increasing concentration, which can be attributed to the stronger dependence of modulus on polymer volume fraction than the linear dependency predicted by the phantom network model. This is due to the fact that at low concentrations there is lower conversion and a higher fraction of connectivity defects, whereas at high concentrations there is more ideal crosslinking with less connectivity defects. Additionally, at high concentrations, entanglements can further increase the modulus. The ratio of phantom to experimental modulus for the PEG–PEG networks in both solvents is lower compared with the PEG–PCL networks and does not decrease with concentration but is rather constant. Here, the scaling with modulus was nearly linear as applied in the phantom model prediction. The lower ratio can be attributed to the slightly higher fraction of single links in these type of networks compared to their amphiphilic analogues and the resulting more ideal network structure.[19]

Overall, the experimentally found values are a factor of maximum 2.4 below the expectation from the phantom network model. This is within reasonable limits, since the networks do not resemble the ideally connected network assumed in the model due to connectivity defects. Furthermore, the experimental system might behave differently compared to the assumptions in the phantom model. Likewise, this is an improvement compared with previous data of PEG–PCL networks in the preparation state[19] and related work based on t-PEG and t-PVDF[18] which reported values a factor of 4 and a factor of 3 below the phantom model expectation, respectively.

Finally, to get an idea about the permeability of the networks for possible guest substances, the mesh size ξ of the networks in the respective solvents can be estimated at $T = 298.15$ K from the plateau modulus G_p in rheology, which corresponds to the experimental found storage modulus G', and the Avogadro-constant N_A as follows[27,46]

$$\xi = \left(\frac{RT}{G' N_A}\right)^{1/3} \quad (2)$$

Figure 9 illustrates that the mesh size decreases with increasing concentration and when switching from non-selective solvent toluene to the selective solvent water. Furthermore, the mesh sizes of the amphiphilic PEG–PCL and the hydrophilic PEG–PEG networks show similar values in the non-selective solvents. This is to be expected, due to the same architecture of the networks, which consist of four-armed star polymers, and the similar molar masses of the building blocks. The trend of the lower swelling of PEG–PEG networks in toluene is also represented here by a slightly lower mesh size.

From a complementary study on the same polymeric system, the mesh size can be roughly estimated from the correlation length in SAXS at the overlap concentration in d_8-toluene, resulting in 4.9 nm and 4.7 nm for PEG–PCL and PEG–PEG networks,

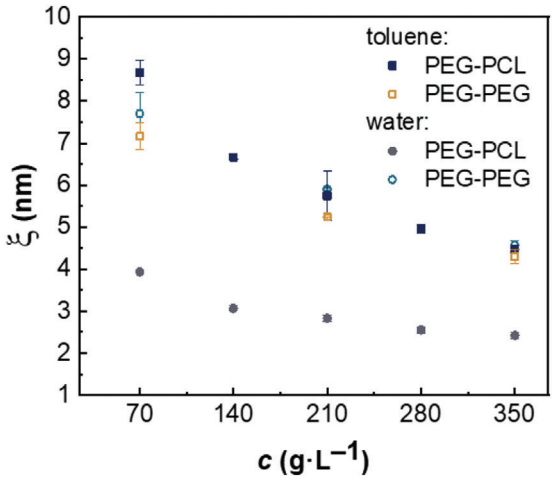

Figure 9. Mesh size as a function of preparation concentration for PEG–PCL (full symbols) and PEG–PEG (open symbols) networks prepared at 25 °C in toluene (dark blue, gold) and water (grey and light blue).

respectively.[25] This is consistent with the trend of smaller mesh size of the PEG–PEG networks compared with the PEG–PCL networks obtained in this work. In addition, the values are in the same order of magnitude, despite different methodologies being used.

2.3.4. Conclusion

In this study, amphiphilic polymer co-networks are prepared by hetero-complementary crosslinking of oxazinone-terminated t-PCL and amino-terminated t-PEG and investigated regarding their environmental sensitive mechanics by AFM and shear rheometry. In addition, they are compared to pure hydrophilic PEG–PEG networks with the same crosslinking chemistry.

As expected, the gelation reaction becomes faster with increasing concentration and temperature. However, the gel points are shifted to longer timescales compared to previous NMR results in d_8-tetrahydrofuran[19] which is attributed to slower kinetics in toluene and the rheometry result as an upper estimate of the gel point.

The equilibrium swelling in the non-selective solvent reveals a concentration dependent swelling degree which follows an apparent scaling law in accord with previous findings and mean field model predictions.[19,20,24] In contrast, the swelling in the selective solvent is constant at a swelling degree of 3, due to a balance in the opposing swelling and shrinking tendencies of the 50:50 mixture of hydrophilic and hydrophobic building blocks. For solvent exchange, a gentle drying procedure at room temperature turns out to be suitable.

The modulus of gels is demonstrated at different length scales by AFM and rheometry, interestingly, showing moduli in the same order of magnitude. This substantiates the picture of homogeneously swollen gels in the non-selective solvent and is further supported by the homogeneous surface structure observed with AFM measurements. For the selective solvent, however, this finding is rather unexpected, since a spherical nano-phase separation can be observed at the surface. Further investigations need to be performed to clarify the role of indenter size and geometry on nanomechanical properties as well as the mechanism by which hard PCL spheres are pushed through the swollen PEG network.

An apparent scaling law of modulus with polymer volume fraction is found. The scaling of the PEG–PCL networks is in accord with previous findings of such networks in a good solvent.[19,21,40,42] However, in water, the scaling is rather linear due to the concentration independent swelling. Such a nearly linear scaling is also found for the PEG–PEG networks in both solvents together with similar mechanical properties.

With this, we demonstrate the precise control of synthesis conditions leading to homogeneous gel networks with defined mechanical properties. This marks a further step towards rationally understanding the interplay between synthesis conditions, the resulting structure and corresponding properties and using this knowledge for the targeted design of functional materials.

3. Experimental Section

Materials: Toluene (≥ 99.5%) was purchased from Fisher Chemical. Milli-Q water was produced in an in-house Milli-Q-system from Merck.

Synthesis of amino-terminated tetra-poly(ethylene glycol) (t-PEG-NH_2) and 2-(4-Nitrophenyl)-benzoxazinone-terminated tetra-poly(ϵ-caprolactone) (t-PCL-Ox)

The synthesis procedure of the tetra-arm star polymers was developed and described by Bunk et al.[19] In general, t-PEG-NH_2 is prepared from t-PEG-OH in a two-step synthesis. First, the mesylate-terminated t-PEG is formed using triethylamine and mesylchloride, which is then converted into the amine-terminated PEG with ammonia. The product is characterized by a narrow molar mass distribution ($Đ$ = 1.02–1.05) and a molar mass of about 10.8 ± 0.2 kg mol^{-1}. t-PCL-Ox is again synthesized in two steps: First, t-PCL-OH is prepared in a ring opening polymerization starting from pentaerythritol. Esterification of t-PCL-OH with 2-(4-Nitrophenyl)−4-oxo-4H-benzo[d][1,3]oxazine-7-carboxylic acid chloride, yields t-PCL-Ox with an oxazinone terminal group as coupling agent. This product in turn is characterized by a narrow molar mass distribution ($Đ$ = 1.07–1.09) and a molar mass of about 11.3 ± 0.2 kg mol^{-1}.

Preparation, Drying and Swelling of Amphiphilic Co-Networks for Rheometry: Stock solutions of t-PEG-NH_2 and t-PCL-Ox at the respective concentrations were prepared in toluene and mixed in equimolar ratio related to the reactive terminal groups. We used concentrations ranging from 70–350 g L^{-1}, corresponding roughly to one to five times the overlap concentration c^*. The mixture was homogenized, poured into a Teflon mold, sealed with a plug, and allowed to react at a constant temperature of 25 or 60 °C for 3 days. The reaction of t-PEG-NH_2 with t-PCL-Ox takes place according to Scheme 1. The resulting gels were detached from the mold and put into an excess of toluene for two days to reach the swelling equilibrium. The swollen networks were weighed directly after the swelling procedure to determine the equilibrium volume swelling degree Q as follows

$$Q = 1 + \left(\frac{\rho_p}{\rho_s}\right)\left(\frac{w_s}{w_p}\right) \quad (3)$$

Here, ρ_p and ρ_s are the density of the polymer and the solvent used, w_p is the weight of the polymer, that is, the dry network, and w_s is the weight of the solvent, that is, the difference of swollen to dried weight. The average density of PEG and PCL is 1.13 g mL^{-1}.[45]

Unless stated otherwise, solvent exchange to a new solvent was carried out via the dry state. For this purpose, the gels were dried at 25 °C at normal pressure for five days to remove the solvent. Subsequently, they were swollen in an excess of the respective new solvent for two days to reach swelling equilibrium.

Preparation of PEG–PEG Networks: Stock solutions of t-PEG-NH_2 and t-PEG-Ox at 70, 210, and 350 g L^{-1} were prepared in toluene and mixed in equimolar ratio related to the reactive terminal groups. The preparation, swelling, and drying procedure is described in detail above. All PEG–PEG networks were prepared at 25 °C. t-PEG-Ox with a molar mass of about 12.5 ± 0.2 kg mol^{-1} was prepared starting from t-PEG-OH according to the procedure described above for synthesis of t-PCL-Ox.

Rheometry: Rheological measurements were carried out with an Anton Paar modular compact rheometer of type MCR302 (Anton Paar, Graz, Austria) equipped with a plate–plate geometry of type PP25 or PP08 with a plate diameter of 25 or 8 mm, respectively. A Peltier plate was used to control the temperature and a solvent trap was utilized to prevent solvent evaporation. The time sweeps for gel point determination were conducted at a constant frequency of $\omega = 6$ rad s^{-1} and a deformation amplitude of $\gamma = 1\%$. Frequency sweeps were carried out at a shear deformation of $\gamma = 0.2\%$ and in the range of $\omega = 0.1$–100 rad s^{-1}.

Viscometry: The intrinsic viscosity [η] of t-PEG-NH_2 in Milli-Q water at 25 °C was determined using an Micro-Ubbelohde Viscometer of Type 537 10/I and the Schulz–Blaschke extrapolation method.[24] The overlap concentration c^* was calculated from the intrinsic viscosity as $c^* = 1/[\eta]$ adapting the same convention as for linear polymers.[47]

Preparation of APCN Gel Films for Atomic Force Microscopy: Additionally, gel samples were prepared for AFM characterization by adding 100 µL of equimolar PEG–PCL polymer mixtures onto amino-functionalized silicon wafers (1 × 1 cm) (Siegert Wafer, Aachen, Germany), for each concentration respectively, resulting in the formation of a gel film. As described previously,[22] APCN gel films were immobilized on the silicon targets which mostly prevents detachment of the sample during the measurements after the addition of excess solvent. Samples were kept in an air-tight container with calculated toluene headspace at 60 °C overnight to complete the reaction. After the completion of the reaction, excess toluene was added to each sample to reach equilibrium swelling degree. For measurements in water, samples were exposed to ambient conditions overnight allowing for the evaporation of toluene. Samples were then re-swollen in water for one day and kept in excess solvent until measurement.

Atomic Force Microscopy: PEG–PCL gels were characterized with atomic force microscopy (AFM). AFM measurements were carried out at room temperature on the MFP3D SA and Cypher (Asylum Research/Oxford Instruments, Wiesbaden, Germany). All measurements were performed in a closed environment with samples in excess solvent and sufficient solvent headspace to prevent solvent evaporation during the measurements. Surface topographies of PEG–PCL gel films were obtained in tapping mode using the cantilevers AC240TSA (70 kHz, 2 N m^{-1}, 7 nm tip radius) or BL-AC40TSA (110 kHz, 0.09 N m^{-1}, 8 nm tip radius) (Oxford, Instruments, Wiesbaden, Germany). Additionally, static indentation measurements were carried out to obtain information about the elastic behavior of gel networks. To investigate different length-scales, cantilevers of different geometries were used. For small scale measurements, the cantilevers CSC38/No Al (10 kHz, 0.03 N m^{-1}) with a tip radius of 8 nm were used. For larger scale measurements, the tipless cantilevers CSC37/tipless/No Al (20 kHz, 0.3 N m^{-1}) and CSC38 tipless/No Al (10 kHz, 0.03 N m^{-1}) with glued and sintered colloidal probes (radius 3.3 µm) were used. All cantilevers used for indentation experiments were fabricated by MikroMasch and purchased from NanoAndMore (Wetzlar, Germany.) Elastic moduli were obtained by recording force maps for tip and colloidal probe measurements on random sample locations to obtain average values and their standard deviations. Force curves were fitted up to an indentation depth of 100 nm using the Hertz model, assuming a Poisson ratio of 0.5. All obtained values were extracted from the AFM in-built software features of IGOR 6.38801 (16.05.191, Asylum research, Santa Barbara, CA, USA).

Supporting Information

Supporting Information is available from the Wiley Online Library or from the author.

Acknowledgements

The authors thank the German Research Foundation (DFG) for funding within the Research Unit FOR2811, "Adaptive Polymer Gels with Model Network Structure" under grant No. 397384169 along with grants 423373052 (TP4), 423768931 (TP5), and 423514254 (TP1).

Open access funding enabled and organized by Projekt DEAL.

Conflict of Interest

The authors declare no conflict of interest.

Data Availability Statement

The data that support the findings of this study are available from the corresponding author upon reasonable request.

Keywords

amphiphilic polymer co-networks, atomic force microscopy, length-scale dependent mechanics, rheology, selective solvent, swelling

Received: October 26, 2023
Revised: November 24, 2023
Published online:

[1] a) G. Erdodi, J. P. Kennedy, *Prog. Polym. Sci.* **2006**, *31*, 1; b) C. S. Patrickios, T. K. Georgiou, *Curr. Opin. Colloid Interface Sci.* **2003**, *8*, 76.
[2] *Amphiphilic Polymer Co-Networks* (Ed.: C. S. Patrickios), Royal Society of Chemistry, Cambridge **2020**.
[3] a) Z. Mutlu, S. Shams Es-Haghi, M. Cakmak, *Adv. Healthcare Mater.* **2019**, *8*, e1801390; b) P. C. Nicolson, J. Vogt, *Biomaterials* **2001**, *22*, 3273;
[4] a) K. Schöller, S. Küpfer, L. Baumann, P. M. Hoyer, D. De Courten, R. M. Rossi, A. Vetushka, M. Wolf, N. Bruns, L. J. Scherer, *Adv. Funct. Mater.* **2014**, *24*, 5194; b) J. Tobis, L. Boch, Y.i Thomann, J. C. Tiller, *J. Membr. Sci.* **2011**, *372*, 219; c) G. Erdodi, J. P. Kennedy, *J. Polym. Sci. A Polym. Chem.* **2005**, *43*, 4965;
[5] P. Grossen, D. Witzigmann, S. Sieber, J. Huwyler, *Journal of Controlled Release* **2017**, *260*, 46.
[6] a) Y.u-Y. Liu, Y.-H. Shao, J. Lü, *Biomaterials* **2006**, *27*, 4016; b) L. Bromberg, M. Temchenko, T. A. Hatton, *Langmuir* **2002**, *18*, 4944; c) M. L. Adams, A. Lavasanifar, G. S. Kwon, *J. Pharm. Sci.* **2003**, *92*, 1343;
[7] G. Lin, L. Cosimbescu, N. J. Karin, A. Gutowska, B. J. Tarasevich, *J. Mater. Chem. B* **2013**, *1*, 1249.
[8] a) H. Wang, Q. Li, J. Yang, J. Guo, X. Ren, Y. Feng, W. Zhang, *J. Mater. Chem. B* **2017**, *5*, 1408; b) R. Murphy, D. P. Walsh, C. A. Hamilton, S.-A. Cryan, M. In Het Panhuis, A. Heise, *Biomacromolecules* **2018**, *19*, 2691;
[9] a) F. Perin, A. Motta, D. Maniglio, *Mater. Sci. Eng. C* **2021**, *123*, 111952; b) A. Dabbaghi, A. Ramazani, N. Farshchi, A. Rezaei, A. Bodaghi, S. Rezayati, *J. Ind. Eng. Chem.* **2021**, *101*, 307; c) M. Shibayama, X. Li, T. Sakai, *Ind. Eng. Chem. Res.* **2018**, *57*, 1121;
[10] T. Sakai, T. Matsunaga, Y. Yamamoto, C. Ito, R. Yoshida, S. Suzuki, N. Sasaki, M. Shibayama, U.-I. L Chung, *Macromolecules* **2008**, *41*, 5379.
[11] Y. Gu, J. Zhao, J. A. Johnson, *Angew. Chem.* **2020**, *59*, 5022.
[12] M. Shibayama, X. Li, T. Sakai, *Colloid Polym. Sci.* **2019**, *297*, 1.
[13] F. Lange, K. Schwenke, M. Kurakazu, Y. Akagi, U.-I.l Chung, M. Lang, J.-U. Sommer, T. Sakai, K. Saalwächter, *Macromolecules* **2011**, *44*, 9666.

[14] S. Nakagawa, N. Yoshie, *Polym. Chem.* **2022**, *13*, 2074.
[15] a) T. Sakai, Y. Akagi, T. Matsunaga, M. Kurakazu, U.-I.l Chung, M. Shibayama, *Macromol. Rapid Commun.* **2010**, *31*, 1954; b) T. Sakai, *React. Funct. Polym.* **2013**, *73*, 898;
[16] T. Hiroi, S. Kondo, T. Sakai, E. P. Gilbert, Y.-S. Han, T.-H. Kim, M. Shibayama, *Macromolecules* **2016**, *49*, 4940.
[17] S. Nakagawa, X. Li, M. Shibayama, H. Kamata, T. Sakai, E. P. Gilbert, *Macromolecules* **2018**, *51*, 6645.
[18] D. E. Apostolides, C. S. Patrickios, T. Sakai, M. Guerre, G. Lopez, B. Améduri, V. Ladmiral, M. Simon, M. Gradzielski, D. Clemens, C. Krumm, J. C. Tiller, B. Ernould, J.-F. Gohy, *Macromolecules* **2018**, *51*, 2476.
[19] C. Bunk, L. Löser, N. Fribiczer, H. Komber, L. Jakisch, R. Scholz, B. Voit, S. Seiffert, K. Saalwächter, M. Lang, F. Böhme, *Macromolecules* **2022**, *55*, 6573.
[20] M. Lang, R. Scholz, L. Löser, C. Bunk, N. Fribiczer, S. Seiffert, F. Böhme, K. Saalwächter, *Macromolecules* **2022**, *55*, 5997.
[21] Y. Akagi, T. Matsunaga, M. Shibayama, U.-I.l Chung, T. Sakai, *Macromolecules* **2010**, *43*, 488.
[22] K. Hagmann, C. Bunk, F. Böhme, R. von Klitzing, *Polymers* **2022**, *14*, 2555.
[23] S. P. O. Danielsen, H. K. Beech, S. Wang, B. M. El-Zaatari, X. Wang, L. Sapir, T. Ouchi, Z.i Wang, P. N. Johnson, Y. Hu, D. J. Lundberg, G. Stoychev, S. L. Craig, J. A. Johnson, J. A. Kalow, B. D. Olsen, M. Rubinstein, *Chem. Rev.* **2021**, *121*, 5042.
[24] J. Bastide, C. Picot, S. Candau, *J. Macromol. Sci., Part B* **1981**, *19*, 13.
[25] L. Löser, C. Bunk, R. Scholz, M. Lang, F. Böhme, K. Saalwächter, *Macromolecules*, under review.
[26] Y. Mai, A. Eisenberg, *Chem. Soc. Rev.* **2012**, *41*, 5969.
[27] M. Rubinstein, R. H. Colby, *Polymer Physics*, 1st ed., Oxford University Press, Oxford **2003**.
[28] a) F. S. Bates, G. H. Fredrickson, *Annu. Rev. Phys. Chem.* **1990**, *41*, 525; b) F. S. Bates, G. H. Fredrickson, *Phys. Today* **1999**, *52*, 32;
[29] W. Burchard, *Branched Polymers II*, Springer, Berlin, Heidelberg **1999**, pp. 113.
[30] E. Merrill, K. Dennison, C. Sung, *Biomaterials* **1993**, *14*, 1117.
[31] T. Matsunaga, T. Sakai, Y. Akagi, U.-I.l Chung, M. Shibayama, *Macromolecules* **2009**, *42*, 6245.
[32] M. Tian, P. Munk, *J. Solution Chem.* **1995**, *24*, 267.
[33] M. Weissmüller, W. Burchard, *Acta Polym.* **1997**, *48*, 571.
[34] K. Shida, K. Ohno, M. Kimura, Y. Kawazoe, Y. Nakamura, *Macromolecules* **1998**, *31*, 2343.
[35] S. Kirincic, C. Klofutar, *Fluid Phase Equilib.* **1999**, *155*, 311.
[36] R. H. Pritchard, E. M. Terentjev, *Polymer* **2013**, *54*, 6954.
[37] a) R. H. Pritchard, P. Lava, D. Debruyne, E. M. Terentjev, *Soft Matter* **2013**, *9*, 6037; b) A. Konda, K. Urayama, T. Takigawa, *Macromolecules* **2011**, *44*, 3000; c) E. Geissler, A. M. Hecht, *Macromolecules* **1980**, *13*, 1276; d) N. Bouklas, R. Huang, *Soft Matter* **2012**, *8*, 8194;
[38] K. Urayama, T. Takigawa, T. Masuda, *Macromolecules* **1993**, *26*, 3092.
[39] a) J. Yoon, S. Cai, Z. Suo, R. C. Hayward, *Soft Matter* **2010**, *6*, 6004; b) F. Di Lorenzo, J. Hellwig, R. Von Klitzing, S. Seiffert, *ACS Macro Lett.* **2015**, *4*, 698;
[40] T. Katashima, K. Urayama, U.-I.l Chung, T. Sakai, *Soft Matter* **2012**, *8*, 8217.
[41] T. Matsunaga, T. Sakai, Y. Akagi, U.-I.l Chung, M. Shibayama, *Macromolecules* **2009**, *42*, 1344.
[42] T. Sakai, M. Kurakazu, Y. Akagi, M. Shibayama, U.-I.l Chung, *Soft Matter* **2012**, *8*, 2730.
[43] B. Lindemann, U. P. Schröder, W. Oppermann, *Macromolecules* **1997**, *30*, 4073.
[44] Y. Akagi, T. Katashima, Y. Katsumoto, K. Fujii, T. Matsunaga, U.-I.l Chung, M. Shibayama, T. Sakai, *Macromolecules* **2011**, *44*, 5817.
[45] Chemical Retrieval on the Web (CROW), Polymer database: Average density of amorphous polymers. http://polymerdatabase.com/polymer%20physics/Polymer%20Density.html (accessed: April 2023).
[46] a) P. Nicolella, M. F. Koziol, L. Löser, K. Saalwächter, M. Ahmadi, S. Seiffert, *Soft Matter* **2022**, *18*, 1071; b) J. Wang, V. M. Ugaz, *Electrophoresis* **2006**, *27*, 3349; c) Y. Tsuji, X. Li, M. Shibayama, *Gels* **2018**, *4*, 50;
[47] G. V. Schulz, F. Blaschke, *J. Prakt. Chem.* **1941**, *158*, 130.